Article

Impacts of Large Dams in the Nan River Basin on the Streamflow and Sediment Supply into the Chao Phraya River, Thailand

Matharit Namsai , Butsawan Bidorn * , Ruetaitip Mama , Warit Charoenlerkthawin

Posted Date: 1 December 2023

doi: 10.20944/preprints202312.0017.v1

Keywords: runoff; environmental impact of dams; sediment transport; hydrological regime; environmental change

Article

Impacts of Large Dams in the Nan River Basin on the Streamflow and Sediment Supply into the Chao Phraya River, Thailand

Matharit Namsai [1,2], Butsawan Bidorn [1,3,*], Ruetaitip Mama [2] and Warit Charoenlerkthawin [1,3]

[1] Department of Water Resources Engineering, Chulalongkorn University, Bangkok 10330, Thailand; Matharit.Na@student.chula.ac.th (M.N.); 6270335121@student.chula.ac.th (W.C.)
[2] The Royal Irrigation Department, Bangkok 10300, Thailand; ruetaitip.mama@gmail.com
[3] Center of Excellence in Interdisciplinary Research for Sustainable Development, Chulalongkorn University, Bangkok 10330, Thailand
* Correspondence: butsawan.p@chula.ac.th; Tel.: +66 2218 6455

Abstract: It was believed that the construction of large dams in the upper tributary basin of the Chao Phraya River (CPR) has caused sediment load reduction in the CPR system by 75–85%. Based on historical and observed river flow and sediment data measured during 1922–2019, we investigated the effects of three large dams, the Sirikit, Naresuan, and Khwae Noi dams, on river runoff and sediment loads supplied to the CPR using Mann-Kendall (MK) test and the double mass curve (DMC). Results from this study revealed that the Nan River contributed approximately 40% and 57% of the runoff and total sediment load (TSL) to the CPR, respectively. The water regulation by the Naresuan diversion dam has mainly caused the reduction on annual runoff and TSL downstream of each dam. The results from this study also reveal that the sediment load observed at the headwater (C.2) of the CPR still increased after the construction of the Sirikit dam due to the expansion of irrigation areas downstream of the dam and the channel improvement in the lower reach of Nan River. After the three major dams were operated, the sediment load at C.2 reduced by 31% compared that discharging during the pre-construction period.

Keywords: runoff; environmental impact of dams; sediment transport; hydrological regime; environmental change

1. Introduction

Rivers are an important link between continents and oceans as they transport large amounts of land-derived materials such as fresh water, sediments, elements, nutrients, and mainly carbon into the global ocean [1–4]. Streamflow and sediment load changes can significantly affect fluvial processes, delta evolutions, and riverine and coastal biogeochemical processes [5,6]. Previous studies suggested that variations in river discharge and sediment load, which are primarily influenced by climate change and human activities, can cause the serious socio-economics consequences [7,8]. During the past several decades, human activities such as deforestation, damming, water diversion, and sand mining have been linked to the changes in runoffs and riverine sediment fluxes [9–13], which directly affect sediment load to the ocean [5,6,14].

Dam is one of the most common structures widely used in water management systems worldwide. However, construction of a dam causes the sediment accumulation in the reservoir, altering river flow and sediment load downstream [15–21]. Significant sediment reduction of 40–98% has been found in many major rivers around the world with insignificant change in annual river runoff due to damming, such as the Three Gorges Dam on the Yangtze River [17,19,22], the High Aswan Dam on the Nile River [9,23], the Hoa Binh Dam on the Red River [15,21], and the Manwan Dam on the Mekong River [18]. However, the effects of dam construction on sediment load in each river depends varies from place to place depending on geological setting, hydrological conditions, dam locations, and water management [24–26]. Since riverine sediment is one of the common sediment sources controlling coastal morphology and shoreline evolution, changes in runoff and

Preprints (www.preprints.org) | NOT PEER-REVIEWED | Posted: 1 December 2023 doi:10.20944/preprints202312.0017.v1

sediment load responding to damming is a crucial information for the sustainable river and coastal management [14,27,28].

The Chao Phraya River (CPR) is a major river of the Greater Chao Phraya River basin, which is the largest river basin in Thailand and the fifth largest in Southeast Asia (Figure 1) [14]. During the past two thousand years, it has delivered fluvial sediments into the Gulf of Thailand, forming the Chao Phraya Delta (CPD) at a progradation rate of 1.5 km^2/y [29]. However, the CPD has experienced severe shoreline retreat over the past six decades with an average recession rate of more than 7 m/y [14,30]. In 1952, the Greater Chao Phraya Project, which was then the most extensive water development project in Asia, was undertaken including the Bhumibol Dam on the Ping River (completed in 1964), the Sirikit Dam on the Nan River (completed in 1972), and many other water distribution systems throughout the Greater Chao Phraya River basin [28]. Based on historical sediment data measured at hydrological station C.2 (Figure 1a), several studies suggested that shoreline recession along the CPD was caused by the construction of two large dams (the Bhumibol and Sirikit Dams) resulting the reduction of annual sediment yield into the CPR by 75–85% [31–34]. Namsai et al. [12] recently reported that the construction of the Bhumibol Dam caused about a 5% reduction in annual sediment supply and no obvious change in the river discharge from the Ping tributary (P.17) to the CPR. Similarly, the construction of three major dams (Kiew Lom, Mae Chang, and Kiew Koh Ma Dams) in the Wang River did not significantly affect streamflow and sediment load of the Wang River (W.4A) into the CPR [25]. Moreover, the sediment load of the Yom River (Stations Y.16) was not affected by the large barrage construction (Mae Yom Barrage) on the mainstream of the river [35].

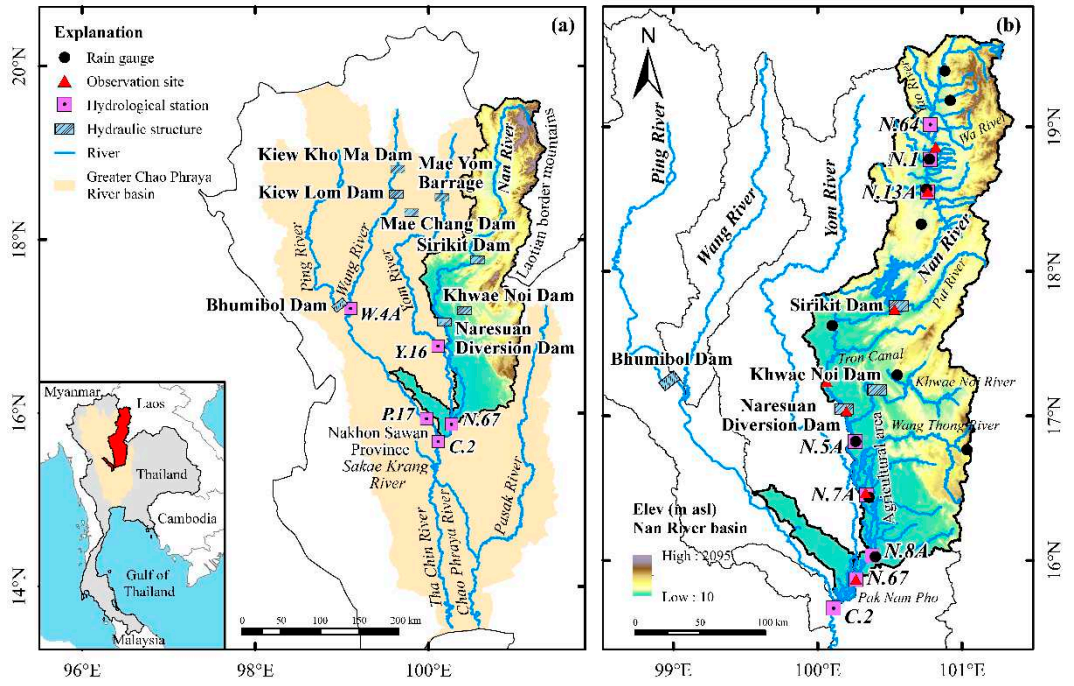

Figure 1. Map of the Greater Chao Phraya River basin, Thailand: (a) Nan River basin and location of major dams in the Chao Phraya River system; (b) locations of hydrological stations operated by the Royal Irrigation Department (RID) and observation sites in this study.

Based on the previous studies, no statistical trend was observed in long-term annual runoff and sediment load supplied from the Ping and Wang Rivers to the CPR [12,25], while the significant increasing trend has been found in the annual runoff and sediment load in the Yom River [35]. However, the long-term sediment load at C.2 of the CPR showed a significant decrease trend [12,25]. Since the Nan River is the largest tributary of CPR, the decline of sediment load at C.2 possibly be caused by some changes in the sediment flux in the Nan River due to large dams in the Nan River basin, such as the Sirikit Dam, Naresuan Diversion Dam, and Khwae Noi Dam. However, sediment

Preprints (www.preprints.org) | NOT PEER-REVIEWED | Posted: 1 December 2023 doi:10.20944/preprints202312.0017.v1

characteristics and variation of sediment load along the Nan River have not been systematically studied yet.

Rivers are highly complex nonlinear dynamic systems [36], and river sediment data are essential to enhance sustainable practices in water resources management and environmental impact assessment. Therefore, the objectives of this study were to (1) investigate the sediment characteristics along the Nan River, (2) analyze the temporal and spatial variations of streamflow and sediment load along the Nan River, and 3) systematically examine the impacts of construction of three major dams (Sirikit, Naresuan Diversion, and Khwae Noi Dams) on runoff and sediment load in the Nan River discharging into the CPR. This study expects to provide a better understanding of the impacts of damming and human activities on sediment transport along the Nan River and CPR system.

2. Materials and Methods

2.1. Study Area

The Nan River basin, which is the largest basin of four major basins (Ping, Wang, Yom, and Nan River basins) forming the CPR system with a drainage area of approximately 34,680 km^2, is located in the northern portion of Thailand, roughly between latitudes 15° 42′ and 18° 37′ N, and from longitudes 99° 51′ to 101° 21′ E [37], as shown in Figure 1a. The north and east basins are bounded by the mountains of the Laotian border, and the split dividing the Yom and Nan River basins is the western boundary of the basin [38]. The Nan River originates in the Luang Phra Bang Mountain (the easternmost range of the Thai highlands) and flows southward through major upper north valleys before traversing the lowland areas in the lower north, merging with the Ping River, and forming the CPR at Pak Nam Pho, Nakhon Sawan Province [39–41] (Figure 1b). The river gradient varies from 1:500 to 1:14,300, as shown in Figure 2, with a mainstream length of approximately 770 km [41–44].

The basin can be divided into three distinct terrain systems, the upper, middle, and lower basins, shown in Figure 2 [37,42]. The upper basin located upstream of the hydrological station N.13A is dominated by mountainous features. The mainstream channel of this portion is 100–200 m wide and 7–12 m deep, while the river slope ranges between 1:500 and 1:3000. Meanwhile, the middle basin is situated between Stations N.13A and N.5A. It is characterized by highland areas with a river gradient from 1:1430 to 1:5000. The river of this portion width varies between 150 and 220 m with a depth between 8 and 10 m. The lower basin located downstream of Station N.5A comprises a floodplain area with a slope of about 1:14,300. The width and depth of the river range between 100 and 150 m and 10 and 17 m, respectively.

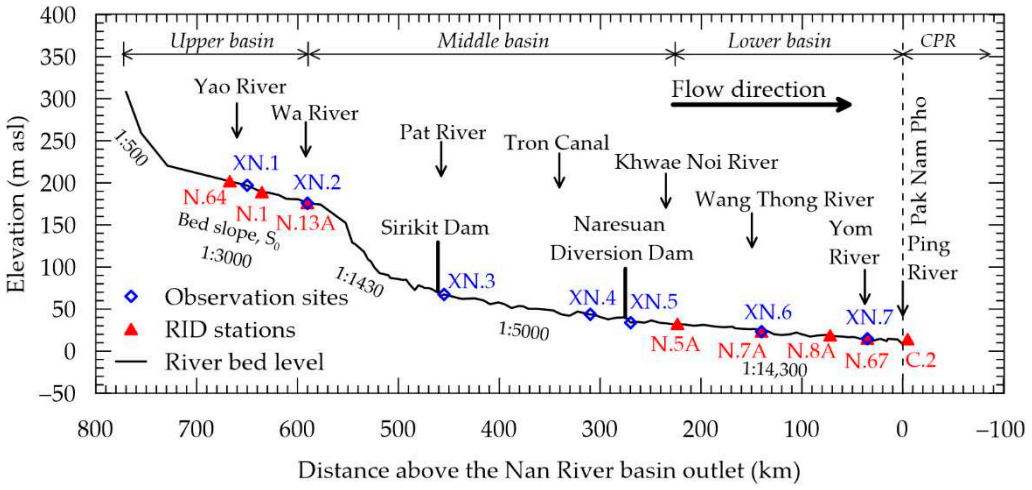

Figure 2. Longitudinal profile of the Nan River showing locations of RID hydrological stations (red triangles) and observation sites (blue diamonds). The zero mark on the x-axis represents the confluence of the Ping and Nan Rivers.

 doi:10.20944/preprints202312.0017.v1

The Nan River basin is also located in a tropical monsoon region. The northeast monsoon influences the climate from November to mid-March causing the dry season, while the wet season is dominated by the southwest monsoon from mid-May to mid-October. The average annual rainfall is 1287 mm, and almost 90% of the total rainfall occurs during the wet season [37]. The average annual runoff is about 12,000 million cubic meters per year ($\times 10^6$ m^3/y), as 38% of the CPR's annual runoff [37]. More than 920 water resources development projects have been constructed in the Nan River basin for irrigation, hydroelectric power generation, flood mitigation, fisheries, and saltwater intrusion control. Three of them are large water resources development projects including the Sirikit Dam, Naresuan Diversion Dam, and Khwae Noi Dam.

The Sirikit Dam located about 460 km from the river basin outlet is the second-largest dam in the CPR system and the third-largest dam in Thailand with normal storage of 9510×10^6 m^3 [37]. The dam was constructed on the middle reach of the Nan River (Figure 1b) and completed in 1972 as a major component of the Greater Chao Phraya Project [45]. The purposes of the dam are for irrigation, hydroelectric power generation, flood mitigation, fisheries, and saltwater intrusion control [46,47]. In 1985, the Naresuan Diversion Dam located approximately 275 km from the river basin outlet was completely constructed in the middle reach to support the water management of the Sirikit Dam, especially diverting water for irrigation purposes [37]. The diversion dam has been used to divert water to the irrigation area and to regulate the river discharge downstream of the diversion dam. In 2011, the Khwae Noi Dam with a normal storage of 939×10^6 m^3 was constructed to mitigate flooding in the Nan River basin and to supply water to some existing agricultural areas, in 2011 on the Khwae Noi River, which is the major tributary of the middle Nan River and located about 240 km upstream of the Nan River basin outlet [48].

2.2. Measurement of River Discharge and Sediment Data

Bedload (BL) and bed material data in Thailand's river are rarely available. Meanwhile suspended sediment load (SSL) data have been collected only at the hydrological stations in some major rivers of the country but generally insufficient for analyzing sediment dynamics. To evaluate the impact of the large dams in the Nan River basin, hydrographic surveys were conducted twice in 2018 (during wet and dry seasons) at 7 sites along the Nan River (XN.1–XN.7 in Figure 2). XN.1 and XN.2 were located on the upper reach, while XN.3–XN.5 and XN.6–XN.7 were situated along the middle and lower reaches, respectively. The measured parameters consisted of river discharge (Q_w), river flow area, flow velocity, water depth, suspended sediment concentration, bedload, and bed material. An Acoustic Doppler Current Profiler (ADCP), Sontek River Surveyor M9 (M9), was used to measure Q_w and river flow area with an accuracy of ±0.25 cm/s for river velocity measurement and 1% for water depth measurement. The flow velocity and water depth measurement resolution were 0.001 m/s and 0.001 m, respectively.

To assess the SSL (Q_s) along the river, at each observation site, a depth-integrating suspended-sediment sampler, US D-49, was utilized to assemble water samples. On the other hand, a US DH-48 was used to obtain samples only when the river section was shallow enough for the investigator to wade across. The river was split into 5–11 sections with equal-width increments for sampling the suspended sediment data. Depth-integrated samples vertical were collected at the center of each increment by lowering the device to reach the riverbed and then immediately raising it to the surface to collect water samples at about 90% of the sampler volume [49]. Water samples were sent to the soil laboratory to analyze suspended sediment concentration described in Namsai et al. [12]. The SSL at each river section was calculated by multiplying the suspended sediment concentration by the corresponding river discharge.

The BL (Q_b) along the Nan River was measured using the standard Helley-Smith (U.S. BL-84) sampler, which is a pressure-different sampler [50]. The sediment samples were collected at the same locations as the suspended sediment sampling, with a sampling period ranging from 1 to 3 min. The samples were sent to a soil laboratory to be dried at 105°C and weighed. Each dried sample was sieved and weighed to determine the distribution of sediment grain using a standard soil particle-size analysis test (ASTM D422). The BL was then determined by calculating, as described in Namsai

Preprints (www.preprints.org) | NOT PEER-REVIEWED | Posted: 1 December 2023 doi:10.20944/preprints202312.0017.v1

et al. [12] and others [51,52]. The bed materials at each site were gathered at the left, middle, and right locations of a river cross-section in this study. A Van Veen grab was used to collect approximately 1–2 kg of surface bed material, with a sampling depth of approximately 20 cm. Each sample was sealed in a plastic bag. All samples were then delivered to a soil laboratory for grain size distribution analysis, which followed the same procedures as the BL sample analysis.

2.3. Detection of Variation and Trend on River Discharge and Sediment Loads

To investigate the variability of river discharge and sediment load along the Nan River, historical daily river discharge and SSL data between 1922 and 2019 were obtained from the RID. Daily streamflow and suspended sediment data were collected at eight hydrological stations (N.64, N.1, N.13A, N.5A, N.7A, N.8A, N.67, and C.2 in Figure 1b). Stations N.64, N.1, and N.13A are in the upper Nan River basin, while Station N.5A is in the middle basin. Moreover, Stations N.7A, N.8A, and N.67 are in the lower basin. In this study, data recorded at Station C.2 (5 km downstream from the confluence of the CPR) was used to assess the effects of the dams on sediment supply from the Nan River to the CPR. Details of river discharge and SSL data at each station are summarized in Table 1. Due to the lack of BL data, the total sediment load (TSL) in the Nan River system was calculated using the sediment rating curves and bed-to-suspended sediment ratios from the river survey data described in Namsai et al. [12].

A non-parametric statistical method, the Mann-Kendall (MK) test, was used to investigate long-term trends in annual streamflow and sediment data along the Nan River [53,54]. The yearly streamflow and sediment data are the sums of daily data between 1st April and 31st March of the consecutive year (Thailand's water year). The MK test has been widely used to determine the significance of trends in skewness and missing data in hydro-meteorological time series [11,55–57]. For a given time series of $X(x_1, x_2, \ldots, x_n)$, the MK statistic, S, is defined as Equation (1).

$$S = \sum_{i=1}^{n-1} \sum_{j=i+1}^{n} sgn(X_j - X_i) \quad (1)$$

where the X_j is the sequential data values, n is the length of the dataset, and sgn(θ) can be calculated using Equation (2).

Table 1. Detailed hydrological record of RID hydrological stations on the Nan River, and Chao Phraya River (CPR).

Station (River)	[1] Dist. (km)	Drainage (km^2)	Data	Period	Max.	Ave.	Min.	[4] S.D.
N.64	+667	3432	[2] Q_w (m^3/s)	1994–2019	2281	82	2	135
(Nan)			[3] Q_s (t/d)	2007–2019	199,765	3053	~0	10,038
N.1	+635	4609	Q_w (m^3/s)	1922–2019	2636	100	1	171
(Nan)			Q_s (t/d)	1978–2019	324,347	2966	~0	12,853
N.13A	+590	8784	Q_w (m^3/s)	1959–2019	4764	197	3	335
(Nan)			Q_s (t/d)	1994–2007	230,624	5593	19	14,138
N.5A	+223	25,286	Q_w (m^3/s)	1951–2019	2159	244	3	263
(Nan)			Q_s (t/d)	1978–2019	141,502	2641	10	6018
N.7A	+140	29,153	Q_w (m^3/s)	1944–2019	1786	320	5	320
(Nan)			Q_s (t/d)	2001–2019	56,373	3566	155	5356
N.8A	+72	31,472	Q_w (m^3/s)	1952–2019	2116	327	1	323
(Nan)			Q_s (t/d)	1997–2019	54,619	3711	135	5015
N.67	+35	57,384	Q_w (m^3/s)	1998–2019	1579	418	33	340

Preprints (www.preprints.org) | NOT PEER-REVIEWED | Posted: 1 December 2023 doi:10.20944/preprints202312.0017.v1

(Nan)			Q_s (t/d)	1999–2019	30,267	5620	84	5904
C.2	–5	109,973	Q_w (m^3/s)	1956–2019	5450	711	15	695
(CPY)			Q_s (t/d)	1965–2019	493,805	13,705	236	27,596

[1] Distance from the Wang River outlet: + sign is distance from the outlet toward upstream; – sign is distance from the outlet toward downstream; [2] Q_w is river discharge (m^3/s); [3] Q_s is suspended sediment load (t/d); [4] S.D. is the standard deviation.

$$sgn(\theta) = \begin{cases} 1, if\ \theta > 0 \\ 0, if\ \theta = 0 \\ -1, if\ \theta < 0 \end{cases} \quad (2)$$

When $n \geq 8$, the statistic S is approximately normally distributed, with the mean and the variance as follows Equations (3) and (4).

$$E[S] = 0 \quad (3)$$

$$V(S) = \frac{n(n-1)(2n+5) - \sum_{i=1}^{n} t_i i(i-1)(2i+5)}{18} \quad (4)$$

where t_i is the number of ties of extent i.

Equations (5) to (7) give the standardized test statistic (z) for the MK test and the corresponding p-value (p) for the one-tailed test.

$$Z = \begin{cases} \frac{S-1}{\sqrt{V(S)}}, if\ S > 0 \\ 0, \quad if\ S = 0 \\ \frac{S+1}{\sqrt{V(S)}}, if\ S < 0 \end{cases} \quad (5)$$

$$p = 0.5 - \Phi(|Z|) \quad (6)$$

$$(\Phi|Z|) = \frac{1}{\sqrt{2\pi}} \int_0^{|Z|} e^{\frac{-t^2}{2}} dt \quad (7)$$

A positive Z value indicates an upward trend, while a negative Z value indicates a downward trend. If $p \leq 0.05$, the existing trend is considered statistically significant at the significance level of 0.05 [55].

2.4. Assessment of the Effects of Large Hydraulic Structure on River Flow and Sediment Load

Double mass curve (DMC) has been most widely used to quantify the contributions of human activities on streamflow and sediment load [17,58]. A DMC is a graph that compares the cumulated values of one variable to another related variable over time [59]. If the two cumulated variables show constant proportionality, a straight line will be plotted, whereas the inflection of the curve represents a change in the constant proportionality or DMC's slope [60].

In this study, the DMCs of cumulative annual rainfall versus cumulative annual runoff were plotted in the prior to and after dam construction to mainly assess the effects of three large dams on yearly runoff along the Nan River. Additionally, the DMCs of cumulative annual river discharge versus cumulative annual TSL were plotted covering pre-and post-dam construction for mostly evaluating the large dams impacts on sediment load along the river. The yearly rainfall data are the sum of daily data for each year (Thailand's water year). The daily rainfall data were analyzed with quality control in account, with data that deviated significantly from historical records being removed and missing data getting interpolated using data from nearby stations or time series. The Thiessen polygon method was used to calculate the catchment-average rainfall for the catchment area of each hydrological station [61].

3. Results

Preprints (www.preprints.org) | NOT PEER-REVIEWED | Posted: 1 December 2023 doi:10.20944/preprints202312.0017.v1

3.1. River Flow and Sediment Characteristics along the Nan River in the 2018 Surveys

River flow and sediment characteristics data along the Nan River observed at XN.1–XN.7 during the dry and wet seasons in 2018 are summarized in Table 2. Meanwhile, the variations of river discharge, SSL, BL, and bed material at each observation site are illustrated in Figure 3. The results from observation at the upper (XN.1 and XN.2), middle (XN.3–XN.5), and lower reaches (XN.6 and XN.7) are summarized as follows.

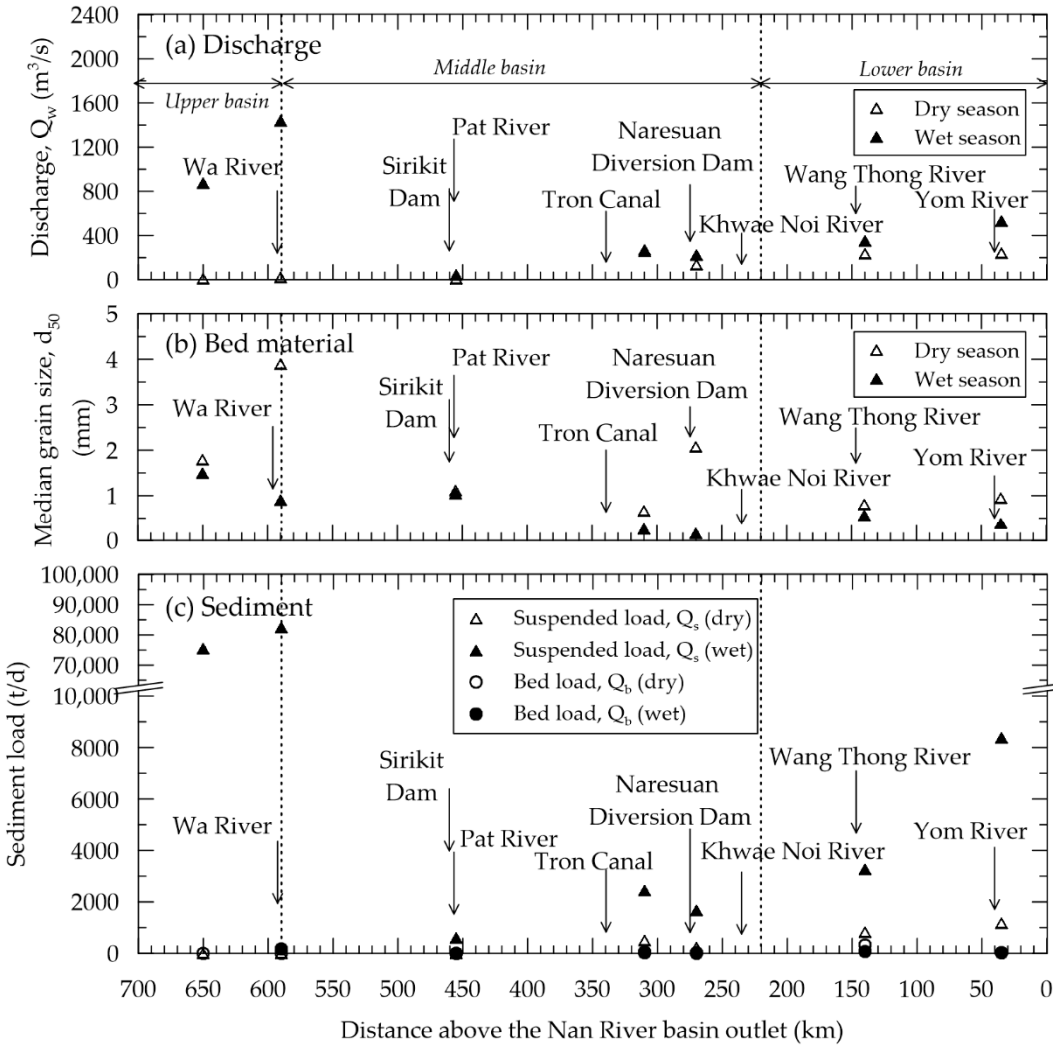

Figure 3. Observations along the Nan River during 2018: (a) river discharge; (b) median size (d_{50}) of bed material; (c) suspended sediment load and bedload.

In the dry season of 2018, the streamflow in the upper Nan River (upstream the Sirikit Dam) increased downstream with a discharge of 8.1–18.1 m^3/s. In the middle course, the river flow between the Sirikit Dam and the Naresuan Diversion Dam rose from 6.7 to 259.2 m^3/s, then declined to 137.7 m^3/s downstream of the Naresuan Diversion Dam. In the lower basin the river flow increased from 236.8 to 241.6 m^3/s (Figure 3a). Figure 3b illustrates that the upper reach was characterized by very coarse sand to very fine gravel, with a median grain size (d_{50}) of 1.79–3.89 mm, while the middle and lower reaches mainly composed of coarse to very coarse sand (d_{50} ranging 0.66–2.07 mm) and coarse sand (d_{50} ranging 0.66–2.07 mm), respectively. In Figure 3c, the observed SSL in the upper basin increased downstream from 6.2 to 7.7 t/d. Similar to the streamflow, the SSL in the middle basin rose toward downstream from 11 to 502 t/d, but the SSL decreased to 229 t/d downstream of Naresuan Diversion Dam. The SSL in the lower basin increased downstream from 814 to 1169 t/d. Table 2 indicated that the BL was below detectable in the upper reach during the dry season. In the middle reach, the BL increased downstream from 0 to 25 t/d. On the other hand, the BL decreased

Preprints (www.preprints.org) | NOT PEER-REVIEWED | Posted: 1 December 2023 doi:10.20944/preprints202312.0017.v1

downstream from 311 to 13 t/d in the lower reach (Figure 3c). The results also indicated that the BL to SSL ratio varied from 0–0.11, and 0.01–0.38 in the middle and lower reaches, respectively (Table 2).

Table 2. Observed streamflow and sediment data along the Nan River in 2018.

Site	Dist. (km)	[1] A (m^2)	[2] V (m/s)	[3] Q_w (m^3/s)	[4] Q_s (t/d)	[5] Q_b (t/d)	[6] Q_t (t/d)	Q_b/Q_s (%)	Q_b/Q_t (%)	d_{50} (mm)
Dry season										
XN.1	650	55	0.15	8.1	6.2	0	6.2	0	0	1.79
XN.2	590	96	0.19	18.1	7.7	0	7.7	0	0	3.89
XN.3	455	143	0.05	6.7	10.8	0	10.8	0	0	1.12
XN.4	310	577	0.45	259.2	501.7	18.4	520.1	3.7	3.5	0.66
XN.5	270	263	0.52	137.7	228.5	24.5	253.0	10.7	9.7	2.07
XN.6	140	302	0.78	236.8	814.2	310.6	1124.8	38.2	27.6	0.80
XN.7	35	478	0.51	241.6	1168.9	12.7	1181.6	1.1	1.1	0.94
Wet season										
XN.1	650	654	1.34	873.4	75,391.8	6.8	75,398.6	~0	~0	1.49
XN.2	590	1512	0.95	1439.8	82,393.2	172.9	82,566.1	0.2	0.2	0.90
XN.3	455	194	0.23	44.6	608.5	0	608.5	0	0	1.05
XN.4	310	523	0.52	272.4	2452.6	45.8	2498.4	1.9	1.8	0.25
XN.5	270	133	1.69	224.7	1681.6	1.5	1683.1	0.1	0.1	0.15
XN.6	140	435	0.80	349.2	3269.6	67.2	3336.8	2.1	2.0	0.56
XN.7	35	656	0.81	532.0	8380.3	22.0	8402.3	0.3	0.3	0.38

[1] A is flow area; [2] V is flow velocity; [3] Q_w is river discharge; [4] Q_s is suspended sediment load; [5] Q_b is bedload; [6] Q_t is total sediment load. d_{50} is median grain size of the bed materials.

The data measured in the wet season indicated that the river flow in the upper basin tended to increase downstream with a flow rate of 873.4–1439.8 m^3/s, then decreased to 45 m^3/s in the middle river reach at XN.3 due to the operation of the Sirikit Dam. The river flow rose to 272.4 m^3/s at XN.4 (upstream of the Naresuan Diversion Dam). However, the streamflow slightly dropped to 224.7 m^3/s downstream of the diversion dam (XN.5). The decrease in the streamflow likely caused by the water diversion upstream of the diversion dam. Meanwhile, the river flow in the lower basin increased from 349.2 to 532 m^3/s from upstream to downstream (Figure 3a). During wet season, the bed material along the Nan River were generally smaller than those compared to the dry season. The upper and middle reaches were defined by coarse to very coarse sand (d_{50} of 0.9–1.49 mm) and fine to very coarse sand (d_{50} of 0.15–1.05 mm), respectively. In the lower reach, the river characterized by medium to coarse sand, with d_{50} ranging between 0.38 and 0.56 mm. Similar to the dry season, the SSL transported along the upper reach increased downstream from 75,392 to 82,393 t/d. In the middle basin, the SSL rose from 609 to 2453 t/d before falling to 1681.6 t/d. However, in the lower basin, the SSL increased from 814 to 1169 t/d (Figure 3b). Unlike in the dry season, in the upper reach, the BL transported at the rate of 7–173 t/d and tended to increase downstream. In the middle reach, the BL increased downstream from 0 to 46 t/d, then fell to 2 t/d downstream of the Naresuan Diversion Dam. The BL decreased downstream from 67 to 22 t/d in the lower reach (Figure 3c). Furthermore, the results showed that the BL to SSL ratio in the upper basin varied 0–0.002. The ratios increased to 0–0.019 and 0.003–0.021 in the middle and lower reaches, respectively (Table 2).

Preprints (www.preprints.org) | NOT PEER-REVIEWED | Posted: 1 December 2023 doi:10.20944/preprints202312.0017.v1

3.2. Historical River Flow and SSL along the Nan River

The statistical analysis of historical daily river discharge and SSL data at several RID hydrological stations from 1922 to 2019 is summarized in Table 1. Additionally, Figure 4 and Figure 5 depict time series of annual streamflow and SSL, respectively.

Figure 4 reveals that the river discharge increased downstream, ranging from 82 m^3/s (N.64) to 418 m^3/s (N.67; 35 km upstream from the river basin outlet). Results from daily river flow analysis (Table 1) also indicated that the river flow in the upper basin increased downstream with the average discharge varying from 82 (N.64) to 197 m^3/s (N.13A). The river discharge raised to 244 m^3/s in the middle basin (N.5A), while the river flow along the lower reach (N.7A, N.8A, and N.67) increased toward downstream with the average flow rate from 320 to 418 m^3/s. The river flow data measured at C.2 (located 5 km downstream the confluence of the Ping and Nan Rivers forming the CPR, Figure 1) indicated that the river discharge notably rose to 711 m^3/s (Table 1).

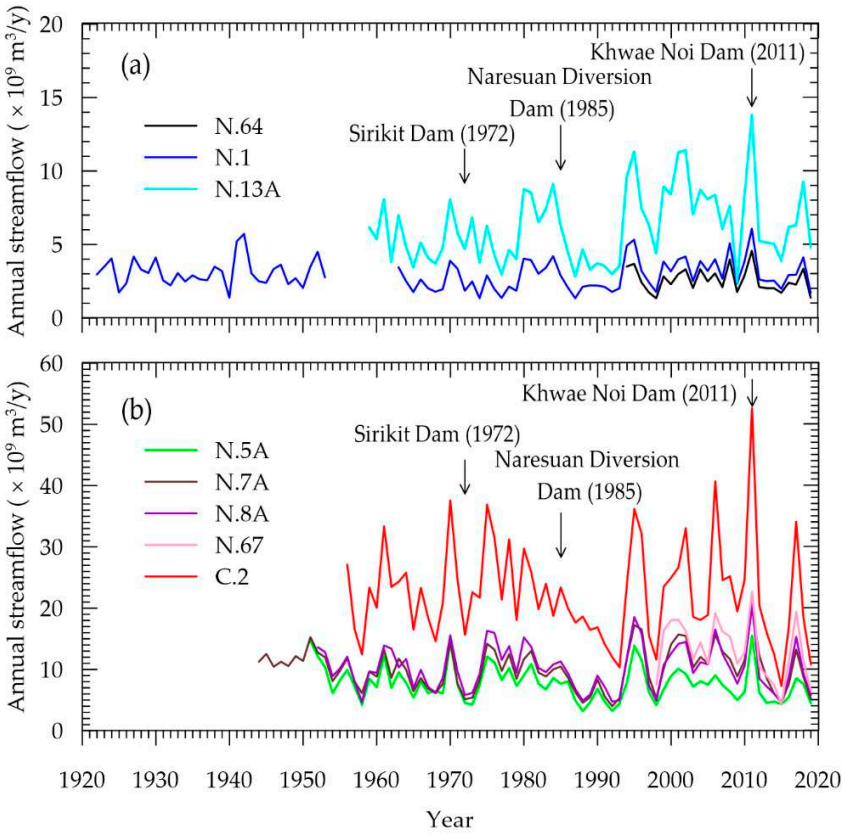

Figure 4. Time series of annual streamflow at the RID hydrological stations between 1922 and 2019: (a) N.64, N.1, and N.13A; (b) N.5A, N.7A, N.8A, N.67, and C.2.

Preprints (www.preprints.org) | NOT PEER-REVIEWED | Posted: 1 December 2023 doi:10.20944/preprints202312.0017.v1

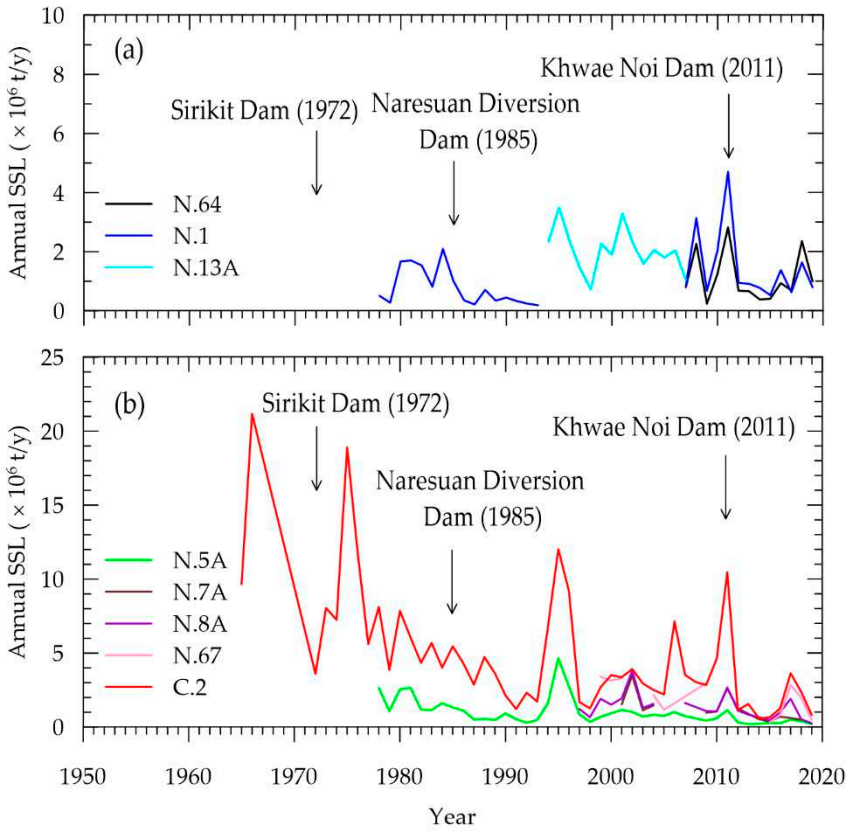

Figure 5. Time series data of annual suspended sediment load at the RID hydrological stations between 1965 and 2019: (a) N.64, N.1, and N.13A; (b) N.5A, N.7A, N.8A, N.67, and C.2.

Based on the results from historical sediment analysis (Table 1), the SSL slightly increased downstream. The average SSL in the upper basin increased from 3053 (N.64) to 5593 t/d (N.13A) but then declined to 2641 t/d in the middle basin (N.5A). In the lower basin, the average SSL observed along the lower reach showed that the average SSL increased downstream from 3566 to 5620 t/d. Meanwhile, the SSL at C.2 averaged 13,700 t/d, which is about 2.4 times higher than average SSL supplied from the Nan River.

By plotting historical daily river flow versus SSL data at each hydrological station, the relationship between SSL and streamflow along the Nan River can be obtained as shown in Figure S1. The plots indicates that the daily SSL along the upper and middle reaches of the Nan River generally had a strong correlation with daily river flow with coefficient of determination (R^2) of greater than 0.82. However, the SSL measured at N.7A, N.8A, N.67, and C.2 (after 1972) had moderate correlation with R^2 between 0.6–0.7 (see Figure S1e,f,g,h). However, statistical values are generally accepted in hydrology analysis when R^2 is greater than 0.5 [62]. Relationships between daily streamflow and SSL analyzed by the linear regression method are presented as Equations (8)–(17):

Station N.64	$Q_s = 0.274Q_w^{1.864}$	$R^2 = 0.82$	(8)
Station N.1	$Q_s = 0.222Q_w^{1.846}$	$R^2 = 0.84$	(9)
Station N.13A	$Q_s = 0.405Q_w^{1.602}$	$R^2 = 0.88$	(10)
Station N.5A (from 1978 to 1997)	$Q_s = 0.062Q_w^{1.946}$	$R^2 = 0.93$	(11)
Station N.5A (from 1998 to 2019)	$Q_s = 0.638Q_w^{1.424}$	$R^2 = 0.58$	(12)
Station N.7A	$Q_s = 1.249Q_w^{1.309}$	$R^2 = 0.60$	(13)
Station N.8A	$Q_s = 2.656Q_w^{1.207}$	$R^2 = 0.63$	(14)

Preprints (www.preprints.org) | NOT PEER-REVIEWED | Posted: 1 December 2023 doi:10.20944/preprints202312.0017.v1

Station N.67 $Q_s = 2.684Q_w^{1.216}$ $R^2 = 0.69$ (15)

Station C.2 (from 1965 to 1971) $Q_s = 0.026Q_w^{2.099}$ $R^2 = 0.89$ (16)

Station C.2 (from 1972 to 2019) $Q_s = 1.221Q_w^{1.316}$ $R^2 = 0.63$ (17)

where Q_s represents daily SSL (t/d), and Q_w represents daily streamflow (m^3/s).

3.3. Variability of Annual Streamflow and Sediment Load along the Nan River

3.3.1. Temporal and Spatial Variation of Annual River Discharge

Results from statistical analysis and MK test on long-term annual streamflow and annual TSL data measured during 1922–2019 are summarized in Table 3. Figure 6 depicts annual river flow and TSL averaged over the considered periods such as 1964–1971 (pre-construction of the Sirikit Dam), 1972–1984 (post-construct Sirikit Dam and pre-construction of Naresuan Diversion Dam), 1985–2010 (post-construction of Naresuan Diversion Dam and pre-construction of Khwae Noi Dam), and 2011–2019 (post-construction of Khwae Noi Dam).

Table 3 shows that the annual streamflow in the upper basin (N.64, N.1, and N.13A) varied from 1.34–13.83 $\times 10^9$ m^3/y without significant increasing of decreasing trend. In contrast, annual runoff in the middle basin (N.5A) ranged 3.20–15.55 $\times 10^9$ m^3/y with a significant decreasing trend. The annual river discharges in the lower basin varied from 4.00 to 22.72 $\times$ 10^9 m^3/y with no significant trend at N.7A and N.8A, but the statistic decreasing trend was found at N.67 near the Nan basin outlet. The annual streamflow at C.2 in CPR ranged 7.30–56.68 $\times$ 10^9 m^3/y without statistical trend (p-values > 0.05). The results also revealed that the significantly higher discharges found at all stations occurred during the flood events, such as in 1995, 2002, 2006, 2011 and 2017 (Figure 4).

Table 3. Results of the Mann-Kendall test for annual streamflow (Q_w) and estimated total sediment load (Q_t) at RID hydrological stations on the Nan River, and Chao Phraya River (CPR) (significance accepted at p-value < 0.05).

Station (River)	[1] Dist. (km)	Drainage (km^2)	Data	Period	Max.	Ave.	Min.	[2] p-Value	[3] Trend
N.64	+667	3432	Q_w ($\times 10^9$ m^3/y)	1994–2019	4.568	2.599	1.338	0.294	Decreasing
(Nan)			Q_t ($\times 10^6$ t/y)		2.826	1.155	0.239	0.760	Decreasing
N.1	+635	4609	Q_w ($\times 10^9$ m^3/y)	1922–2019	6.079	2.964	1.342	0.893	Decreasing
(Nan)			Q_t ($\times 10^6$ t/y)		4.733	1.158	0.188	0.929	Decreasing
N.13A	+590	8784	Q_w ($\times 10^9$ m^3/y)	1959–2019	13.830	6.211	2.384	0.093	Increasing
(Nan)			Q_t ($\times 10^6$ t/y)		4.528	1.400	0.258	0.218	Increasing
N.5A	+223	25,286	Q_w ($\times 10^9$ m^3/y)	1951–2019	15.548	7.709	3.199	**0.027**	**Decreasing**
(Nan)			Q_t ($\times 10^6$ t/y)		6.882	1.767	0.299	**<0.0001**	**Decreasing**
N.7A	+140	29,153	Q_w ($\times 10^9$ m^3/y)	1944–2019	20.119	10.104	4.001	0.578	Decreasing
(Nan)			Q_t ($\times 10^6$ t/y)		4.176	1.261	0.344	0.087	Decreasing
N.8A	+72	31,472	Q_w ($\times 10^9$ m^3/y)	1952–2019	20.801	10.308	4.608	0.525	Decreasing
(Nan)			Q_t ($\times 10^6$ t/y)		3.833	1.239	0.254	0.564	Decreasing
N.67	+35	57,384	Q_w ($\times 10^9$ m^3/y)	1998–2019	22.725	13.185	4.264	**0.048**	**Decreasing**
(Nan)			Q_t ($\times 10^6$ t/y)		3.435	1.875	0.313	**0.021**	**Decreasing**
C.2	–5	109,973	Q_w ($\times 10^9$ m^3/y)	1956–2019	52.675	22.437	7.296	0.313	Decreasing
(CPY)			Q_t ($\times 10^6$ t/y)		21.811	4.825	0.600	**0.003**	**Decreasing**

[1] Distance from the Wang River outlet: + sign is the distance from the outlet toward upstream; – sign is the distance from the outlet toward downstream; [2] p-value; [3] trend refer to the Mann-Kendall test; statistically significant trend is marked as bold text.

Preprints (www.preprints.org) | NOT PEER-REVIEWED | Posted: 1 December 2023 doi:10.20944/preprints202312.0017.v1

Based on the average annual river flow (Table 3), the stream flow in the Nan River increased toward downstream from 2.6×10^9 m^3/y at the headwater to 13.2×10^9 m^3/y at the outlet, while the river flow at C.2 averaged 22.44×10^9 m^3/y. Figure 6a illustrates the average annual runoff during the pre- and post-construction of major hydraulic structures (Sirikit Dam, Naresuan Diversion Dam, and Khwae Noi Dam) along the Nan River. It was found that average annual runoff significantly increased from upstream to downstream (Figure 6a). The results also revealed that the average annual runoff along the Nan River before Sirikit Dam construction (1963–1971) was lower than that after the construction of the dam (1972–1984). After the construction of Naresusn Diversion Dam in 1985, the average annual runoff during 1985–2010 observed at the stations (N.5A, N.7A, N.8A, N.67, and C.2) downstream of the Sirikit Dam was obviously lower than that before the construction of the diversion dam, even though the average annual streamflow at stations upstream of the dam (N.1, N.13A) increased. Figure 6a also shows that the construction of Khwae Noi Dam in the Khwae Noi River, a major tributary of the Nan River, did not obviously affect the river runoff in the lower reach of Nan River (N.7A and N.8A). Based on the comparison on average river discharge between the outlet of the Nan River basin (N.8A) and the headwater of the CPR (C.2), the water discharged from the Nan River accounted for about 60% of the CPR's runoff (Figure 4).

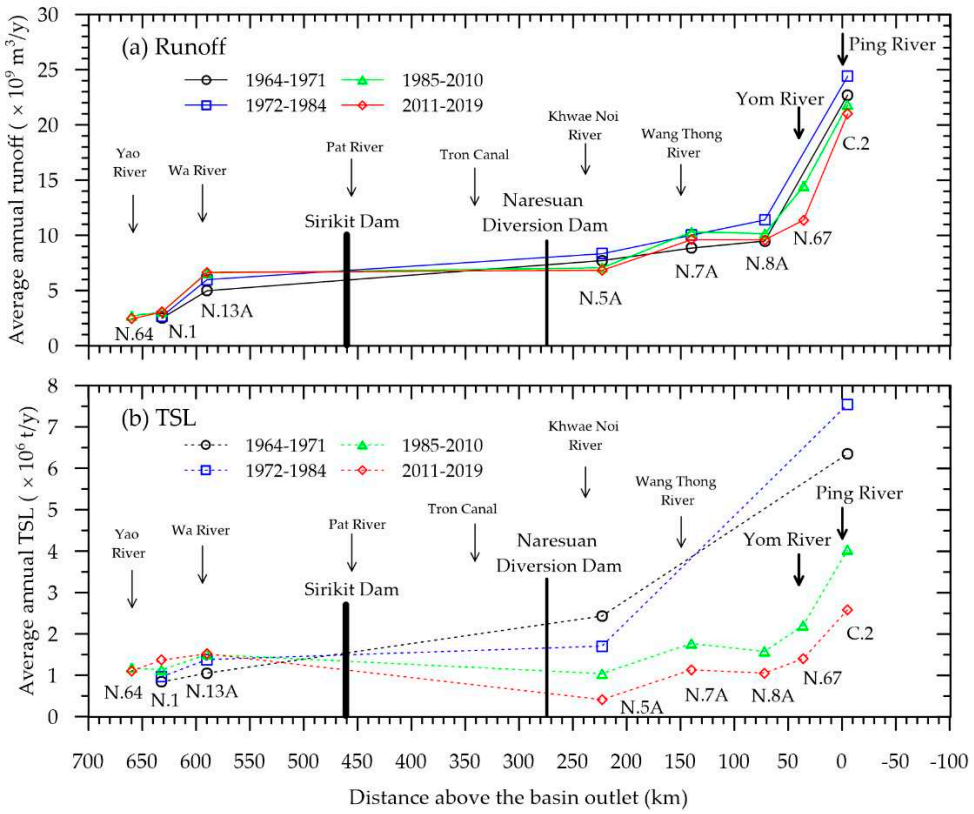

Figure 6. Plots of (**a**) average annual river runoff and (**b**) annual total sediment load (TSL) along the Nan River.

3.3.2. Temporal and Spatial Variation of Annual TSL

The sum of SSL and BL represents the TSL transported along the Nan River. To evaluate the variability of sediment load along the Nan River, including the effects of damming on sediment loads in this river and sediment supply to the CPR system, the TSL at each hydrological station was estimated. Because measured SSL data were discontinuous and available only in some locations for a few recent decades, the relationship between river discharge and SSL at each station (Equations (8)–(17)) were used to estimate missing daily SSL data during the past decades. Then, the BL to SSL ratios BL obtained from our field surveys was used to estimate the BL corresponding to daily SSL data. In this study, the long-term BLs at N.5A, N.7A, N.8A, and N.67 were calculated using the BL to SSL

Preprints (www.preprints.org) | NOT PEER-REVIEWED | Posted: 1 December 2023 doi:10.20944/preprints202312.0017.v1

ratios of 0.05, 0.20, 0.20, and 0.01, respectively, whereas the BLs in the upper basin (N.64, N.1, and N.13A) were very low (~0). Moreover, the BL to SSL ratio of 0.03 studied by Bidorn et al. [63] was used to estimate the BL of C.2. Figure 7 depicts the estimated annual TSL in the upper, middle, and lower reaches of the Nan River during 1922–2019, and the results from basic statistics and trend analyses of annual TSL data are summarized in Table 3.

Based on the results from MK test (Table 3), no significant trend (p-values < 0.05) has been found in annual TSL at N.64, N.1, N.13A, N.7A, and N.8A, whereas significant decreasing trend has been found in annual TSL at N.5A and N.67 (p-values < 0.05). In the upper and middle basin, the annual TSLs varied from 0.19–4.73 × 10^6 t/y and from 0.30 to 6.88 × 10^6 t/y, respectively. In the lower basin, the annual TSLs varied from 0.25 to 4.18 × 10^6 t/y. Meanwhile, the annual TSL data at C.2 ranged 0.6–21.811 × 10^6 t/y with a significant decreasing trend (p-values < 0.05). The results indicated that the annual TSLs of all stations were noticeably high during flood events, like those in 1995, 2002, 2006, 2011 and 2017 (Figure 7).

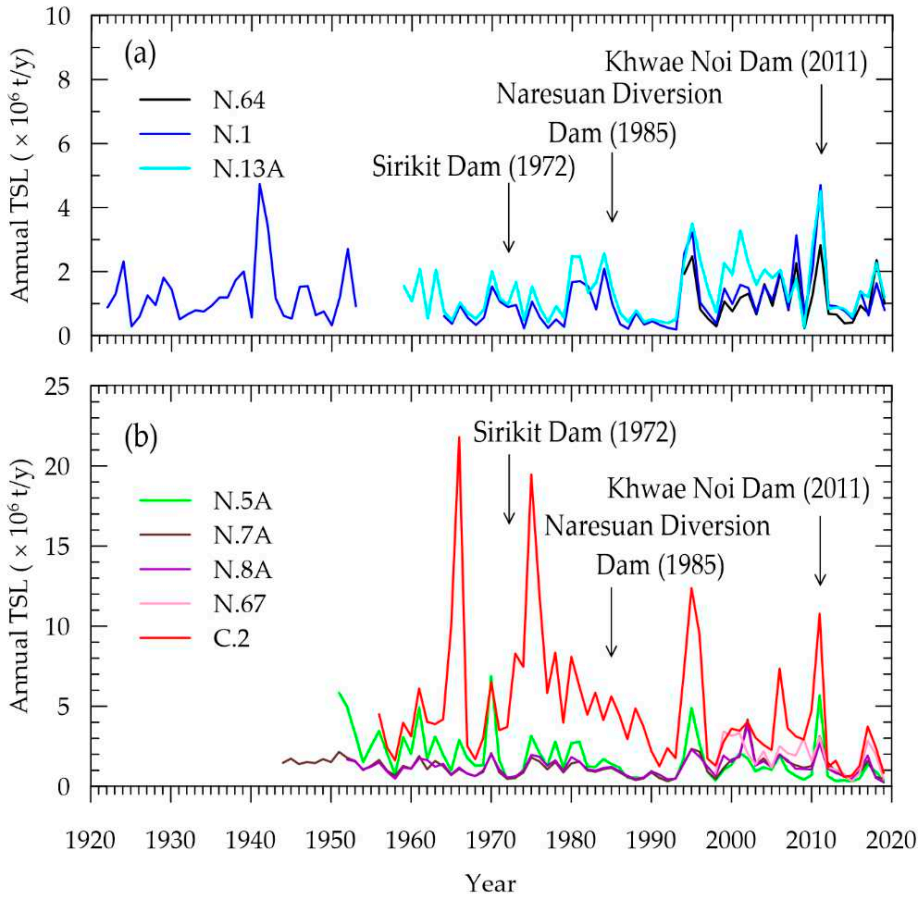

Figure 7. Time series data of annual total sediment load (TSL) at the RID hydrological stations between 1922 and 2019: (a) N.64, N.1, and N.m13A; (b) N.5A, N.7A, N.8A, N.67, and C.2.

The spatial variation analysis of annual TSL revealed that the average long-term annual TSLs at N.64, N.1, N.13A, N.5A, N.7A, N.8A, N.67, and C.2 were 1.155, 1.158, 1.400, 1.669, 1.476, 1.372, 1.875, and 4.825 × 10^6 t/y, respectively (Table 3). Unlike the annual river discharge, the average annual TSLs after the dams' building fluctuated along the river. In the river upstream of the Sirikit Dam, the average sediment load of all time periods (1964–1971, 1972–1984, 1985–2010, and 2011–2019) increased upstream to downstream (Figure 6b). Meanwhile, the average annual TSLs downstream of the Sirikit Dam rose along the river (Figure 6b). However, the average yearly TSL of N.7A was greater than N.8A after the construction of the Naresuan Diversion Dam in 1985. Additionally, the averages annual sediment load of all time periods significantly climbed at C.2 (Figure 6b). Based on Figure 6b, prior to the construction of the Sirikit and Naresuan Diversion Dams, there was an observed increase

Preprints (www.preprints.org) | NOT PEER-REVIEWED | Posted: 1 December 2023 doi:10.20944/preprints202312.0017.v1

in the average annual sediment load along the river from upper to lower reaches. The data reveal that the average annual TSLs at N.1 and N.13A, located upstream of the Sirikit Dam, were higher during 1972–2019 compared to the pre-dam construction period of 1964–1971. Furthermore, post-construction observations indicate a significant reduction in average annual TSL at N.5A: a 30% decrease following the construction of the Sirikit Dam (1972–1984), a 57% decrease post-Naresuan Dam (1985–2010), and an 83% decrease following the Khwae Noi Dam (2011–2019). Conversely, the average annual TSL at Station C.2 exhibited an initial increase of 17% during 1972–1984, followed by reductions of 40% and 61% in the periods 1985–2010 and 2010–2019, respectively. The sediment data reveals that average annual TSL at N.67 between 1998 and 2019 accounted for 70% of the C.2 (Figure 7).

3.4. Effects of Three Large Dams on Streamflow and Sediment Load along the Nan River

3.4.1. Effects of the Dams on the Annual Streamflow

To assess the effects of the Sirikit Dam, Naresuan Diversion Dam, and Khwae Noi Dam dams on streamflow and sediment loads in rivers, a double mass curve (DMC) of cumulative annual rainfall and cumulative annual runoff as well as cumulative annual runoff and cumulative annual TSL were used. Figures 8 and 9 depict the DMCs of annual rainfall versus annual runoff and annual runoff versus TSL at six stations along the Nan River over 1944–2019.

Figure 8 revealed that the DMC slope of the stations located along the Nan River (Figure 8a–e) wavered during 1975–1994, while the DMC slope of C.2 slightly decreased during 1985–1994. The shift of DMC slope at all stations were found in 2011 due to the Thailand great flood of 2011.

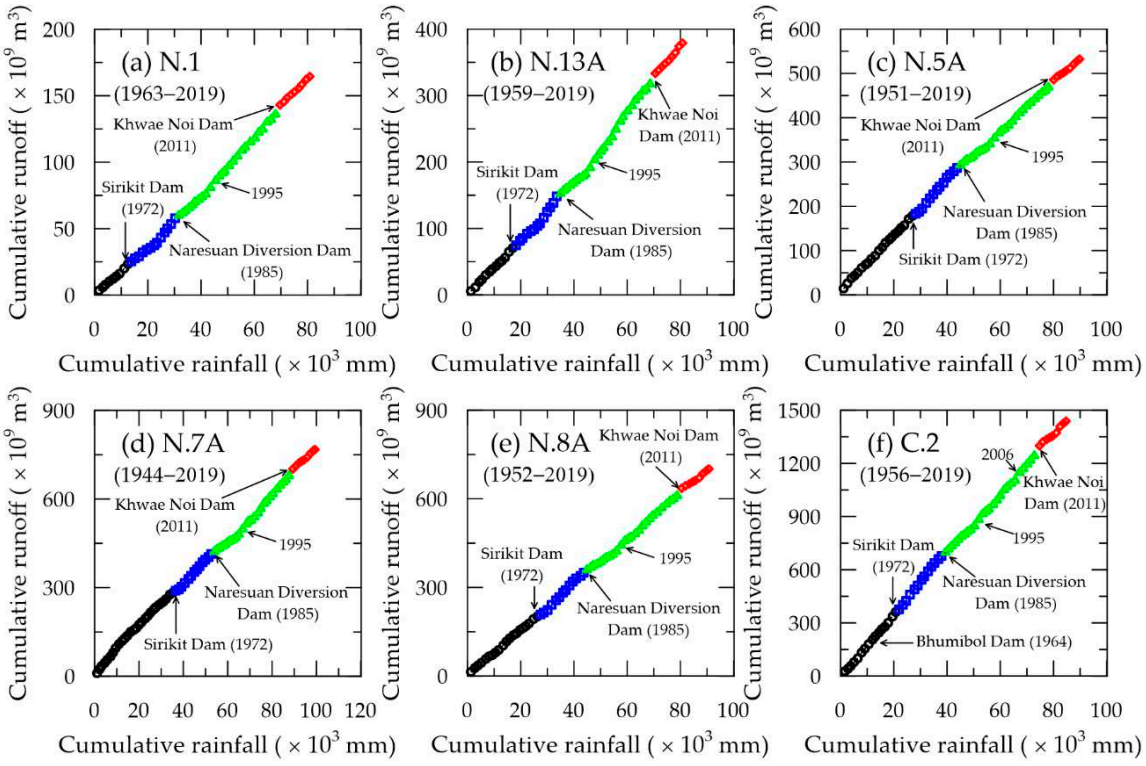

Figure 8. Plots showing cumulative annual rainfall and runoff of the Nan River: (**a**) N.1; (**b**) N.13A; (**c**) N.5A; (**d**) N.7A; (**e**) N.8A; (**f**) C.2; black, blue, green, and red points represent data during pre-construction of the Sirikit Dam, pre-construction of the Naresuan Diversion Dam, pre-construction of the Khwae Noi Dam, and post-construction of the Khwae Noi Dam, respectively.

Preprints (www.preprints.org) | NOT PEER-REVIEWED | Posted: 1 December 2023 doi:10.20944/preprints202312.0017.v1

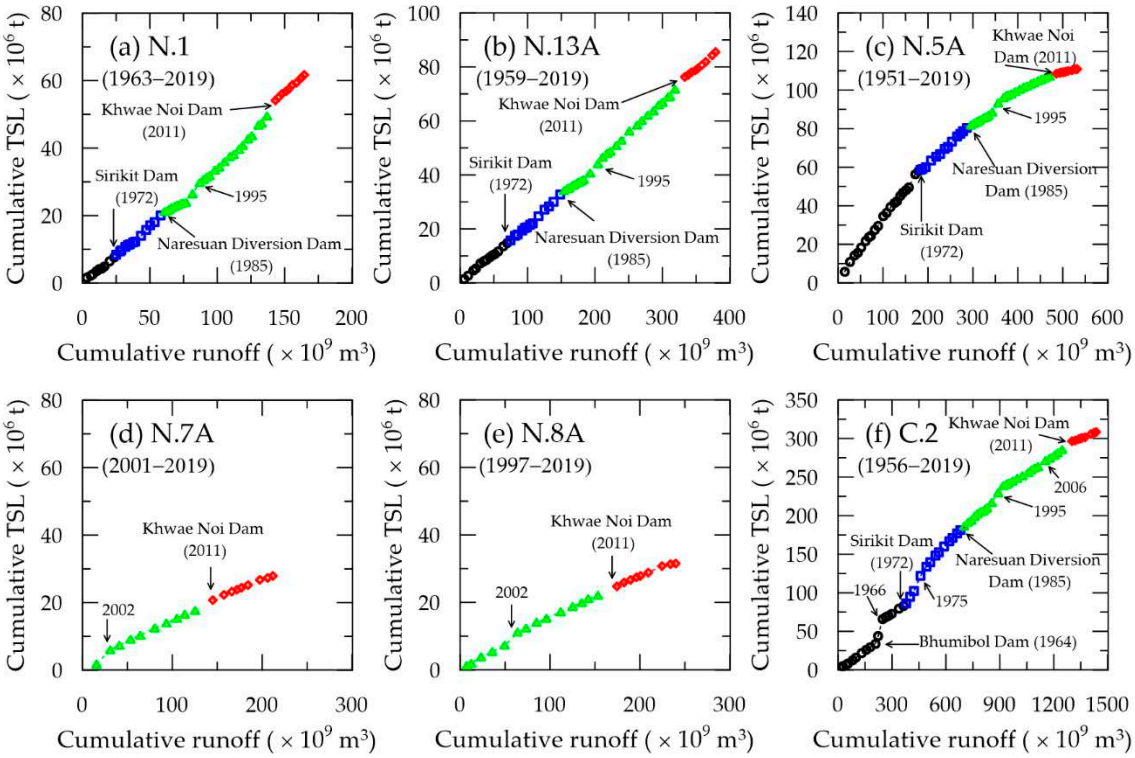

Figure 9. Plots showing cumulative annual runoff and TSL of the Nan River: (**a**) N.1; (**b**) N.13A; (**c**) N.5A; (**d**) N.7A; (**e**) N.8A; (**f**) C.2; black, blue, green, and red points represent data during pre-construction of the Sirikit Dam, pre-construction of the Naresuan Diversion Dam, pre-construction of the Khwae Noi Dam, and post-construction of the Khwae Noi Dam, respectively.

3.4.2. Effects of the Dams on the Annual TSL

Figure 9 illustrates the plots of DMCs of annual runoff and annual TSL, which illustrate the effect of three dam construction on sediment load along the Nan River and sediment supply to the CPR. The DMC's slope of N.1 and N.13 (Figure 9a,b) indicate that the sediment load in the upper reach of the Nan River (upstream the Sirikit Dam) varied regarding the change in river runoff pattern during 1975–1994. In contrast, the reduction of the DMC's slope of N.5A (Figure 9c) located in the middle basin (downstream of dams were found after 1972 for a couple years, followed by the increase slope during 1975–1984. The decline slope was found at N.5A again since 1985 (after the construction of the Naresuan diversion dam). Meanwhile, the DMC plots of N.7A and N.8A located in the lower basin (Figure 9d,e) show insignificant change of the slope during 1997–2019. Figure 9f illustrated the DMC at C.2, which notable increase slope was found during 1972–1995, and the slope slightly declines after 1996.

4. Discussion

4.1. Sediment Characteristics along the Nan River

The Nan River is one of four major tributaries (Ping, Wang, Yom, and Nan Rivers) forming the CPR, but the sediment transport characteristics along the river have never been thoroughly studied and documented [37]. Based on the observed sediment data in 2018 (Table 2), the upper Nan River (gradient 1:3000) contained coarse sand to fine gravel, the middle reach (gradient less than 1:5000) had fine to very coarse sand, and the lower reach (1:14,300) comprised medium to coarse sand. Although all tributaries of the upper CPR basin are neighboring and are similar in terms of climate [12,25,64], the bed materials of each river were different. The Nan River's bed material, which contains larger size of sediment than other tributaries, possibly was influenced by the operation of the major Sirikit, Naresuan Diversion, and Khwae Noi Dams. The clear water released from the dams has a high potential to move fine sediment from the riverbed. Therefore, the

 doi:10.20944/preprints202312.0017.v1

The Nan River's TSL is mostly suspended sediment, similar to the Yom River but different from the Ping and Wang Rivers. Downstream of the Bhumibol Dam, the SSLs in the Ping River fluctuate between 2% and 70% of the TSL [12]. In the Wang River, following the Kiew Koh Ma and Kiew Lom Dams, SSLs constitute 20% to 22% of the TSL [25]. Conversely, in the Nan River, below the Sirikit Dam, SSLs comprise a higher percentage, ranging from 72% to 100% of the TSL. This is attributed to the Sirikit Dam's role in sediment trapping and the accumulation occurring upstream of the Naresuan Diversion Dam. Downstream of the diversion dam, reduced river flow decreases the ability to transport bed sediment at each cross-section. The increase in SSL is due to fine sediments from major tributaries (Pat River, Tron Canal, Khwae Noi River, Wang Thong River, Yom River) and nearby agricultural areas (Figure 1b). This increase and the change in flow dynamics diminish the correlation between daily SSL and river discharge in the lower Nan River and CPR (N.5A, N.7A, N.8A, N.67, and C.2), as depicted in Figure S1. The moderate correlation between daily SSL and discharge results from decreased flow velocity, attributable to a lower river gradient (Figure 2), leading to significant sedimentation in the lower reaches [42]. A similar weak correlation between daily SSL and runoff is observed in the lower Yom River [35] and the lower Yangtze River [17].

In non-mountainous rivers (gradient flatter than 1:500), BL typically makes up 10–20% of TSL, while in mountainous rivers (gradient steeper than 1:500), it's about 20–30% [65]. In Thailand, the Royal Irrigation Department (RID) estimates BL as 30% of SSL or 23% of TSL for water resource projects [66]. However, in the Nan River, despite some mountainous sections, the river's gradient classifies it as non-mountainous (Figure 2). This study found BL in the upper, middle, and lower Nan River to be 0–0.2%, 0–9.7%, and 0.1–27.6% of TSL, respectively, differing from traditional estimates due to dam regulation and irrigation projects [65]. In the upper Nan basin, BL is lower than expected as TSL is mostly in suspension including the wash load dominates SSL. Riverbed slope changes from 1:500 to 1:3000 reduce flow velocity and sediment transport, causing deposition [42]. Small dams in the upper basin may trap BL from tributaries [37]. Similar low BLs are found in the upper reaches of the Ping, Wang, and Yom Rivers [12,25,35]. In contrast, BLs in the middle and lower Nan River increase due to dam operations, with BLs downstream of the Bhumibol Dam in the Ping River exceeding 80% of TSL [12], and those in the Wang River affected by the Kiew Koh Ma and Kiew Lom Dams reaching 78–80% of TSL [25]. In the Yom River, without large dams, BLs in the middle and lower reaches are under 5% of TSL [35].

The study's results show that sediment characteristics vary significantly across different rivers and even within different reaches of the same river, highlighting their area-specific nature. Consequently, consistent and ongoing monitoring is essential to gather accurate sediment data, which is crucial for effective and sustainable water resource management and development.

4.2. Runoff and Sediment Load Dynamics along the Nan River

Climate factors and human activities, particularly rainfall, influence runoff and sediment load variability [19,22,67]. The Mann-Kendall (MK) analysis of streamflow in the upper Nan River basin showed no significant trend in annual runoff (p-value > 0.05), suggesting that climate, especially rainfall, dominates discharge variations here [8,11,56]. However, a declining trend in streamflow was observed in the middle reach at station N.5A (p-value = 0.027), likely due to the Naresuan Diversion Dam impacts, as evidenced by the reduction in the DMC of cumulative rainfall and discharge between 1985 and 2011 (Figure 8c). In the lower river, no significant streamflow decrease was found at stations N.7A, N.8A, and C.2, although the DMCs indicated a decreased slope after 1985 and 2011 (Figure 8d,e,f). This also suggests the Naresuan Diversion may have influenced the lower-reach flow reduction, while tributaries and irrigation canals might have compensated the runoff. Additionally, Station N.67 showed a significant decline trend in streamflow (MK test, p-value = 0.048), reflecting the Naresuan Diversion Dam's impact. High streamflow during flood years (1966, 1975, 1995, 2002, 2006, 2011, 2017) contrasted with a declining trend in 1981–1993 across all stations, mirroring a low-water period in Thailand [35].

Analysis of average daily water discharge and yearly runoff at various stations showed an increase in discharge downstream along the Nan River, correlating with catchment area expansion.

 doi:10.20944/preprints202312.0017.v1

From 1972–1984, post-Sirikit Dam and pre-Naresuan Diversion Dam, annual streamflow increased more than in the 1964–1971 pre-Sirikit Dam period, attributed to increased rainfall [57]. However, post-1985, post-Naresuan Diversion Dam, average annual discharge upstream of the Sirikit Dam continued to rise, while it decreased downstream due to the Naresuan Diversion and Khwae Noi Dams' operations. The impact of the Khwae Noi Dam on streamflow was minimal, as storage dams typically release yearly discharge downstream close to natural conditions (Figure S2a,c). Notably, yearly runoff at station N.7A exceeded that at N.8A after 1985, likely due to side flow from irrigation canals and the Wang Thong River (Figure 6a, S3).

Sediment analysis (Table 3, Figure 7a) indicates no significant trend in the TSL of the upper Nan River basin (MK test, p-value > 0.05), paralleling streamflow patterns. The DMCs for cumulative annual runoff and TSL at stations N.1 and N.13A also showed no significant changes from 1922–2019 (Figure 9a,b), linking TSL variations to river discharges. However, the middle river (N.5A) displayed a marked decline in annual TSL (MK test, p-value < 0.0001), with significant DMC slope reductions since 1985 (Figure 9c), influenced by the operation of the Naresuan diversion dam since 1985, and post-1995 flood management structures. In the lower basin, a significant TSL decrease at stations N.7A, N.8A, and N.67 (p-value < 0.05) was noted. Contrastingly, the C.2 station in the Chao Phraya River showed a significant TSL decrease, with notable high TSL during flood years like 1995, 2002, 2006, and 2011 (Figure 7). Since construction of storage dams in the Ping, Wang, and Nan seems insignificantly reduced sediment loads at the river outlets, the decrease in sediment load found at C.2 during the past several decades may be caused by the changes in sediment regime due to water regulation, which intensely operated to support irrigation activities [30,41,63].

Spatial variation analysis revealed an increase in average annual TSL from upstream to downstream in the upper Nan River (Figure 6b), similar to patterns in the upper Ping River [12] and upper Yangtze River, China [8]. Downstream of the Sirikit Dam, TSL fluctuated due to large dam operations. Post-1985, TSL rose in the lower Nan River (N.7A) due to sediment influx from irrigation canals and the Wang Thong River (Figure S3), but decreased in N.8A, a sediment sink area. Sedimentation and annual dredging by the Marine Department (200,000–700,000 m^3/y) contribute to TSL reduction in the lower reaches [39,42]. However, TSL at N.67 increased, potentially influenced by sediment from the Yom River, agricultural areas, and drainage canals. At C.2 in the Chao Phraya River, TSL significantly increased due to contributions from the Yom and Ping Rivers (Figure 6b).

4.3. Effects of Large Dams on Runoff and Sediment Load along the Nan River

The impact of large dams on riverine streamflow and sediment supply has been widely reported [3,10,24,33,68–70]. The Three Gorges Dam, for example, significantly reduced sediment load in the Yangtze River, affecting its delta [5,8,17,22,36]. Similarly, the effects of dams in the Chao Phraya River basin (including Ping, Wang, Yom, and Nan Rivers) on sediment load have been studied due to coastal erosion in the upper Gulf of Thailand [12,25,31–34]. However, the Bhumibol Dam on the Ping River did not affect the river's streamflow and sediment load [12], nor did the dams in the Wang River basin and the barrage on the Yom River [25,35].

This study found that while the Sirikit Dam on the Nan River (completed in 1972) didn't change annual runoff, the Naresuan Diversion did, as indicated by the declining slope of the Double Mass Curve (DMC) of annual rainfall and runoff post-1985 (Figure 8c,d,e) [37,48]. The outflow of the Naresuan Diversion Dam into the mainstream varied between 43-77% of the inflow, altering water extracted from the river [37]. Large storage dams had a minimal impact on annual streamflow due to their operation balancing the ecosystem downstream [71].

The study also showed a decline in TSL downstream of the Sirikit Dam after the construction of the three dams, as sediment was trapped in reservoirs and diverted for irrigation, leading to sediment deposition upstream of the diversion dam (Figure 9c,d,e) [26,47]. Despite this, sediment load increased in the lower Nan River due to agricultural activities and contributions from tributaries and irrigation areas, with sediment loss from rice cultivation estimated at 4.32×10^6 t/y [37,72]. The movement of bed load downstream of the dams also contributed to changes in river processes (Table 2).

Preprints (www.preprints.org) | NOT PEER-REVIEWED | Posted: 1 December 2023 doi:10.20944/preprints202312.0017.v1

4.4. Impacts of Major Dams on Runoff and Sediment Supply into the CPR

The streamflow and sediment supply into the CPR system were assessed at station C.2, summarizing the Ping and Nan Rivers' contributions. C.2's average annual streamflow was 22.473 x 10^9 m^3/year with no trend, while its TSL significantly decreased to 4.83 x 10^6 t/y, particularly after the construction of three large dams in the Nan River basin (Figure 7, Table 3). Annual river discharge and TSL data (1954-2019) at P.17 (Ping River), N.67 (Nan River), and C.2 showed that N.67 and P.17 contributed 60% and 35% to C.2's runoff, respectively (Figure 10a). The Yom River (Y.16) contributed about 33% to N.67's discharge, equating to 20% of C.2's flow, while the Wang River basin provided about 15% and 5% to P.17's and C.2's runoff, respectively [25,35]. The Nan (N.67) and Ping (P.17) Rivers accounted for 70% and 26% of the CPR's annual TSL at C.2 (Figure 10b). The sediment concentration was higher in the Nan River, especially during the wet season (Figures S4, S5). Therefore, the Nan River basin emerged as the largest contributor of both water (40%) and sediment (57%) to the CPR system.

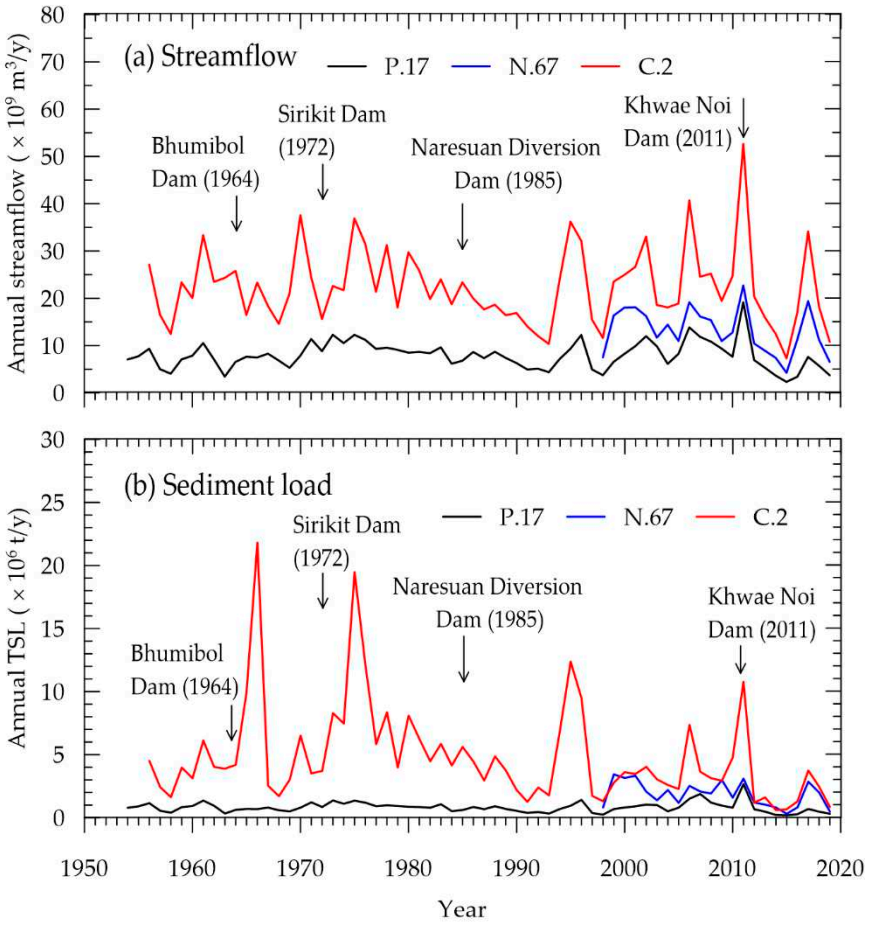

Figure 10. Time series data of annual streamflow (a) and total sediment load (b) at the RID hydrological stations P.17, N.67, and C.2 between 1954 and 2019.

The construction of the Naresuan Diversion and Khwae Noi Dams resulted in reduced annual streamflow in the Chao Phraya River (CPR), as shown by the decreased slope of the cumulative annual rainfall and runoff DMC at station C.2 after 1985 and 2011 (Figure 8f). This reduction was due to the diversion of Nan River flow for irrigation by the Naresuan Diversion Dam (Figure S2b) and water allocation from the Khwae Noi Dam to nearby irrigation areas [48]. These dams also significantly lowered the annual TSL in the CPR, indicated by the reduced DMC slope of cumulative annual runoff and TSL post-1985 and 2011 (Figure 9f), with sediment either being trapped or redirected to irrigation areas.

 doi:10.20944/preprints202312.0017.v1

In contrast, TSL at C.2 increased after the 1972 construction of the Sirikit Dam (Figure 9f). While this dam trapped upstream sediment, downstream agricultural expansion [37,40] and intensified rice cultivation (2-3 crops/year) in the Nan River basin [72] led to increased sediment loads, contributing around 4.32 x 10^6 t/y to the downstream Nan River (Figure S3). These changes, coupled with improvements by the Royal Irrigation Department (RID) in the lower Nan River during 1973-1975 [73], boosted sediment load after 1972.

The remote location of the Sirikit Dam from C.2 (465 km) meant its impact on TSL and streamflow at C.2 was minimal. The Kiew Lom Dam on the Wang River also had little effect on TSL at the river basin outlet due to its downstream agricultural expansion [25]. Conversely, the Bhumibol Dam slightly reduced TSL after 1966 (Figure 9f) due to sediment trapping, with increased sedimentation downstream from expanded irrigation (approximately 97,600 ha). Soil loss from agricultural activities in the lower Ping River basin added approximately 2.135×10^6 t/y of sediment (Figure 9f) [72]. The TSL increase during 1964-1966 was influenced by the RID's river enhancements and agricultural growth following the Bhumibol Dam's construction [73].

The study revealed a significant decrease in the slope of the DMC at station C.2 post-1995, attributed to the construction of additional hydraulic structures for flood control and agricultural water supply in the lower Ping, Yom, and Nan River basins, along with extensive dredging in the lower Nan River downstream of N.67, which removed approximately 360,000–1,260,000 t of sediment annually [25,42] (Figure 9f). This increase in cross-sectional area reduced flow velocity and sediment transport, leading to more sediment deposition before reaching the CPR. Generally, large dams trap most upstream sediment [74], reducing TSL downstream, yet their role in altering sediment load at river basin outlets is significant. The expansion of irrigation and agricultural areas following the construction of the Sirikit and Bhumibol Dams substantially increased TSL at C.2, whereas the Khwae Noi Dam and other flood control structures significantly decreased it, a pattern similar to sediment load reductions in major rivers like the Yangtze [8], Yellow [56], and Nile [23] due to dam constructions. Compared to earlier studies at C.2, this analysis found only a 31% reduction in CPR sediment load post-2011, as opposed to the 75–85% reduction observed in the pre-1995 period, before the construction of these mega-dams [31–34,44] (Figure 9f).

5. Conclusions

In this study, we examined sediment characteristics, streamflow variation, and the impact of three large dams in the Nan River basin on the runoff and sediment load in the Nan River and the Chao Phraya River (CPR) at C.2. Our findings indicate that the Nan River is a significant contributor to the CPR, providing 40% of the water outflow and 57% of the TSL. The river, primarily an alluvial system with fine sand to very fine gravel, transports most sediment in suspension. Notably, the Naresuan Diversion Dam obviously led to a decrease in both runoff and TSL in the Nan River, particularly downstream, while the Sirikit Dam primarily reduced TSL. Post-construction of the Bhumibol and Sirikit Dams, TSL at C.2 increased due to expanded irrigation and agricultural activities downstream, contrasting with the decline after 1985 due to intensive water regulation in the upper CPR basin. The sediment load at C.2 decreased by only 31% post-dam construction compared to the pre-dam period (1956–1963). This study underscores the nuanced impact of dam construction on river basin sediment dynamics, revealing how dams for irrigation expansion can increase sediment load, while those for flood control and water use can decrease it. These findings offer valuable insights for sustainable food and water management in developing countries, amidst the environmental challenges of large-scale reservoir projects.

Supplementary Materials: The following supporting information can be downloaded at the website of this paper posted on Preprints.org. Figure S1: Sediment rating curves at eight RID hydrological stations: (a) N.64; (b) N.1; (c) N.13A; (d) N.5A; (e) N.7A; (f) N.8A; (g) N.67; (h) C.2, Figure S2: Annual inflow and outflow of dams (a) Sirikit Dam; (b) Naresuan Diversion Dam; (c) Khwae Noi Dam, Figure S3: The streamflow and sediment supply into the middle and lower reaches of the Nan River from the tributaries and drainage canals, Figure S4: Comparison between the concentration of sediment in the Ping and Nan Rivers: (a) 1985; (b) 2003; (c) 2010; (d)

2014; (e) 2017; (f) 2020, and Figure S5: Comparison between the sediment concentration in the Yom and Nan Rivers: (a) 2008; (b) 2010; (c) 2014; (d) 2017; (e) 2018; (f) 2020.

Author Contributions: Conceptualization, M.N. and B.B.; methodology, M.N. and R.M.; formal analysis, M.N., B.B. and R.M.; investigation, B.B., M.N., and W.C.; resources, R.M.; data curation, M.N. and R.M.; writing—original draft preparation, M.N.; writing—review and editing, B.B.; visualization, M.N. and W.C.; supervision, B.B.; project administration, B.B.; funding acquisition, B.B. All authors have read and agreed to the published version of the manuscript.

Funding: This research was funded by Chulalongkorn University, grant number GB-B_62_011_21_05 and Office of the Higher Education Policy, Science, Research, and Innovation National Council (NRCT) by Human Resource Development and Management Unit and Funding for the Development of Higher Education Institutions Research and Innovation Creation, grant number B05F630024.

Data Availability Statement: The data presented in this study is available on request from the corresponding author.

Acknowledgments: The authors acknowledge the support of the RID for providing the river datasets used in this study. The authors also acknowledge the support of the 100th Anniversary Chulalongkorn University Fund for Doctoral Scholarship, the 90th Anniversary Chulalongkorn University Fund (Ratchadaphiseksomphot Endowment Fund: GCUGR1125633037D) and Research Assistant Scholarship (GCUGE17).

Conflicts of Interest: The authors declare no conflict of interest.

References

1. Peng, J.; Chen, S.L.; Dong, P. Temporal variation of sediment load in the Yellow River basin. *CATENA* **2010**, *2*, 135–147.
2. Wang, H.J.; Saito, Y.S.K.; Zhang, Y.; Bi, N.S.; Sun, X.X.; Yang, Z.S. Recent changes of sediment flux to the western Pacific Ocean from major rivers in East and Southeast Asia. *Earth-Science Reviews* **2011**, *108*, 80–100.
3. Liu, S.W.; Zhang, X.F.; Xu, Q.X.; Liu, D.C.; Yuan, J.; Wang, M.L. Variation and driving factors of water discharge and sediment load in different regions of the Jinsha River basin in China in the past 50 years. *Water* **2019**, *11*, 1109.
4. Das, S. Dynamics of streamflow and sediment load in Peninsular India rivers. *Science of The Total Environment* **2021**, *799*, 149372.
5. Zhang, X.; Dong, Z.; Gupta, H.; Wu, G.; Li, D. Impact of the Three Gorges Dam on the hydrology and ecology of the Yangtze River. *Water* **2016**, *8*, 590.
6. Liu, C.; He, Y.; Li, Z.; Chen, J.; Li, Z. Key drivers of changes in the sediment loads of Chinese rivers discharging to the oceans. *International Journal of Sediment Research* **2021**, *36*, 747–755.
7. Guo, P.; Geissen, V.; Ritsema, C.J.; Mu, X.M.; Wang, F. Impact of climate change and anthropogenic activities on streamflow and sediment discharge in the Wei River basin, China. *Hydrology and Earth System Sciences* **2013**, *17*, 961–972.
8. Zhao, Y.; Zou, X.; Liu, Q.; Yao, Y.; Li, Y.; Wu, X.; Wang, C.; Yu, W.; Wang, T. Assessing natural and anthropogenic influences on water discharge and sediment load in the Yangtze River, China. *Science of The Total Environment* **2017**, *607–608*, 920–932.
9. Walling, D.E.; Fang, D. Recent trends in the suspended sediment loads of the world's rivers. *Global and Planetary Change* **2003**, *39*, 111–126.
10. Walling, D.E. Human impact on land-ocean sediment transfer by the world's rivers. *Geomorphology* **2006**, *79*, 192–216.
11. Jiang, C.; Zhang, L.; Li, D.; Li, F. Water discharge and sediment load changes in China: Change patterns, causes, and implications. *Water* **2015**, *7*, 5849–5875.
12. Namsai, M.; Charoenlerkthawin, W.; Sirapojanakul, S.; Burnett, W.C.; Bidorn, B. Did the construction of the Bhumibol Dam cause a dramatic reduction in sediment supply to the Chao Phraya River? *Water* **2021**, *13*, 386.
13. Tessler, Z.D.; Vörösmarty, C.J.; Grossberg, M.; Gladkova, I.; Aizenman, H.; Syvitski, J.P.M.; Georgiou, E.F. Profiling risk and sustainability in coastal deltas of the world. *Science* **2015**, *349*, 638–643.
14. Bidorn, B.; Sok, K.; Bidorn, K.; Burnett, W.C. An analysis of the factors responsible for the shoreline retreat of the Chao Phraya Delta (Thailand). *Science of The Total Environment* **2021**, *769*, 145253.

15. Lu, X.X.; Oeurng, C.; Le, T.P.Q.; Thuy, D.T. Sediment budget as affected by construction of a sequence of dams in the lower Red River, Viet Nam. *Geomorphology* **2015**, *248*, 125–133.
16. Guo, L.; Su, N.; Zhu, C.; He, Q. How have the river discharges and sediment loads changed in the Changjiang River Basin downstream of the Three Gorges Dam? *Journal of Hydrology* **2018**, *560*, 259–274.
17. Yang, H.F.; Yang, S.L.; Xu, K.H.; Milliman, J.D.; Wang, H.; Yang, Z.; Chen, Z.; Zhang, C.Y. Human impacts on sediment in the Yangtze River: A review and new perspectives. *Global and Planetary Change* **2018**, *162*, 8–17.
18. Binh, V.D.; Kantoush, S.; Sumi, T. Changes to long-term discharge and sediment loads in the Vietnamese Mekong Delta caused by upstream dams. *Geomorphology* **2020**, *353*, 107011.
19. Guo, C.; Jin, Z.; Guo, L.; Lu, J.; Ren, S.; Zhou, Y. On the cumulative dam impact in the upper Changjiang River: Streamflow and sediment load changes. *CATENA* **2020**, *184*, 104250.
20. Reisenbüchler, M.; Bui, M.D.; Rutschmann, P. Reservoir sediment management using artificial neural networks: A case study of the lower section of the Alpine Saalach River. *Water* **2021**, *13*, 818.
21. Ve, N.D.; Fan, D.; Van Vuong, B.; Lan, T.D. Sediment budget and morphological change in the Red River Delta under increasing human interferences. *Marine Geology* **2021**, *431*, 106379.
22. Tian, Q.; Xu, K.H.; Dong, C.M.; Yang S.L.; He, Y.J.; Shi, B.W. Declining sediment discharge in the Yangtze River from 1956 to 2017: Spatial and temporal changes and their causes. *Water Resources Research* **2021**, *57*, e2020WR028645.
23. Shalash, S. Effects of sedimentation on the storage capacity of the High Aswan Dam reservoir. Hydrobiologia 1982, 91, 623–639.
24. Wu, Z.; Zhao, D.; Syvitski, J.P.M.; Saito, Y.; Zhou, J.; Wang, M. Anthropogenic impacts on the decreasing sediment loads of nine major rivers in China, 1954–2015. *Science of The Total Environment* **2020**, *739*, 139653.
25. Charoenlerkthawin, W.; Namsai, M.; Bidorn, K.; Rukvichai, C.; Panneerselvam, B.; Bidorn, B. Effects of dam construction in the Wang River on sediment regimes in the Chao Phraya River basin. *Water* **2021**, *13*, 2146.
26. Chong, X.Y.; Vericat, D.; Batalla, R.J.; Teo, F.Y.; Lee, K.S.P.; Gibbins, C.N. A review of the impacts of dams on the hydromorphology of tropical rivers. *Science of The Total Environment* **2021**, *794*, 148686.
27. Bidorn, B.; Phanomphongphaisarn, N.; Rukvichai, C.; Kongsawadworakul, P. Evolution of mangrove muddy coast in the Western Coast of the Upper Gulf of Thailand over the past six decades. In *Estuaries and Coastal Zones in Times of Global Change*, Springer Water; Nguyen, K., Guillou, S., Gourbesville, P., Thiébot, J., Eds.; Springer: Singapore, 2020; pp. 429–442.
28. Vongvissessomjai, S. Chao Phraya Delta: Paddy field irrigation areas in tidal deposits. In Proceedings of the 56th International Executive Council of ICID, Beijing, China, 10–18 September 2005. Available online: https://www.rid.go.th/thaicid/_5_article/2549/10_1ChaoPhraYaDelta.pdf (accessed on 13 April 2021).
29. Tanabe, S.; Saito, Y.; Sato, Y.; Suzuki, Y.; Sinsakul, S.; Tiyapairach, S.; Chaimanee, N. Stratigraphy and Holocene evolution of the mud-dominated Chao Phraya delta, Thailand. *Quaternary Science Reviews* **2003**, *22*, 789–807.
30. Charoenlerkthawin, W.; Bidorn, K.; Burnett, W.C.; Sasaki, J.; Panneerselvam, B.; Bidorn, B. Effectiveness of grey and green engineered solutions for protecting the low-lying muddy coast of the Chao Phraya Delta, Thailand. *Scientific Reports* **2022**, *12*, 20448.
31. Winterwerp, J.C.; Borst, W.G.; De Vries, M.B. Pilot study on the erosion and rehabilitation of a mangrove mud coast. *Journal of Coastal Research* **2005**, *21*, 223–230.
32. Uehara, K.; Sojisuporn, P.; Saito, Y.; Jarupongsakul, T. Erosion and accretion processes in a muddy dissipative coast, the Chao Phraya River delta, Thailand. *Earth Surface Processes and Landforms* **2010**, *35*, 1701–1711.
33. Milliman, J.D.; Farnsworth, K.L. *River Discharge to the Coastal Ocean: A Global Synthesis*; Cambridge University Press: New York, NY, USA, 2011; pp. 1–382.
34. Gupta, H.; Kao, S.J.; Dai, M. The role of mega dams in reducing sediment fluxes: A case study of large Asian rivers. *Journal of Hydrology* **2012**, *464–465*, 447–458.
35. Namsai, M.; Bidorn, B.; Chanyotha, S.; Mama, R.; Phanomphongphaisarn, N. Sediment dynamics and temporal variation of runoff in the Yom River, Thailand. International Journal of Sediment Research 2020, 35, 365–376.
36. Wang, Y.; Rhoads, B.L.; Wang, D.; Wu, J.; Zhang, X. Impacts of large dams on the complexity of suspended sediment dynamics in the Yangtze River. *Journal of Hydrology* **2018**, *558*, 184–195.

37. Hydro and Agro Informatics Institute (HAII). *Report on Data Collection and Analysis: Database Development Project and Flood and Drought Modeling of 25 River Basins (Nan River Basin)*; Hydro and Agro Informatics Institute: Bangkok, Thailand, 2012. (In Thai)
38. Royal Irrigation Department (RID). *Nan River Basin Hydrometeorological Report*; Royal Irrigation Department: Bangkok, Thailand, 1969.
39. Bidorn, B.; Kish, S.A.; Donoghue, J.F.; Bidorn, K.; Mama, R. Change in sediment characteristics and sediment load of the Nan River due to large dam construction. In Proceedings of the 37th IAHR World Congress 2017, Kuala Lumpur, Malaysia, 13–18 August 2017; IAHR: Kuala Lumpur, Malaysia, 2017; pp. 403–412.
40. Hydro and Agro Informatics Institute (HAII). *Report on Data Collection and Analysis: Database Development Project and Flood and Drought Modeling of 25 River Basins (Ping River Basin)*; Hydro and Agro Informatics Institute: Bangkok, Thailand, 2012. (In Thai)
41. Office of Natural Resources and Environmental Policy and Planning (ONEP). *Developing Watershed Management Organizations in Pilot Sub-Basins of the Ping River Basin*, Final Report; Office of Natural Resources and Environmental Policy and Planning, Ministry of Natural Resources and Environment: Bangkok, Thailand, 2005.
42. Marine Department (MD). *The Feasibility Study of River Navigation, Port, Revetment for Rivers in the North and North-East of Thailand: Nan River*; Marine Department: Bangkok, Thailand, 2002. (In Thai)
43. Electricity Generating Authority of Thailand (EGAT). *Sediment survey of Sirikit Dam*; Report No. 31303-3603; Electricity Generating Authority of Thailand: Bangkok, Thailand, 1993.
44. Japan International Cooperation Agency (JICA). *The Feasibility Study on Mangrove Revival and Extension Project in the Kingdom of Thailand*; Final Report; Ministry of Agriculture: Bangkok, Thailand, 2001.
45. Japan International Cooperation Agency (JICA). *Project for the Comprehensive Flood Management Plan for the Chao Phraya River Basin*; Final Report; Office of National Economic and Social Development Board: Bangkok, Thailand, 2013.
46. Royal Irrigation Department (RID). *Nan River Project Feasibility Report Multipurpose Project, Irrigation, Power, Flood Control, and Navigation*; Royal Irrigation Department: Bangkok, Thailand, 1964.
47. Royal Irrigation Department (RID). *Nan River Basin Development Feasibility Report Uttaradit Irrigation Project and Phitsanulok Irrigation Project*; Royal Irrigation Department: Bangkok, Thailand, 1970.
48. Royal Irrigation Department (RID). *A Study of Dam Break Project of Khwae Noi Dam, Phitsanulok Province*; Royal Irrigation Department: Bangkok, Thailand, 2009. (In Thai)
49. Edwards, T.K.; Glysson, G.D.; Guy, H.P.; Norman, V.W. *Field Methods for Measurement of Fluvial Sediment*; US Geological Survey: Denver, CO, USA, 1999; pp. 1–89.
50. Helley, E.J.; Smith, W. *Development and Calibration of a Pressure-Difference Bedload Sampler*; US Department of the Interior, Geological Survey, Water Resources Division: Menlo Park, CA, USA, 1971; pp. 1–18.
51. Lemma, H.; Nyssen, J.; Frankl, A.; Poesen, J.; Adgo, E.; Billi, P. Bedload transport measurements in the Gilgel Abay River, Lake Tana Basin, Ethiopia. *Journal of Hydrology* **2019**, *577*, 123968.
52. Rachlewicz, G.; Zwoliński, Z.; Kociuba, W.; Stawska, M. Field testing of three bedload samplers' efficiency in a gravel-bed river, Spitsbergen. *Geomorphology* **2017**, *287*, 90–100.
53. Kendall, M.G. *Rank Correlation Methods*, 4th ed.; Charles Griffin: London, UK, 1975.
54. Mann, H.B. Nonparametric tests against trend. *Econometrica* **1945**, *13*, 245–259.
55. Yue, S.; Wang, C. The Mann-Kendall test modified by effective sample size to detect trend in serially correlated hydrological series. *Water Resources Management* **2004**, *18*, 201–218.
56. Shi, H.; Hu, C.; Wang, Y.; Liu, C.; Li, H. Analyses of trends and causes for variations in runoff and sediment load of the Yellow River. *International Journal of Sediment Research* **2017**, *32*, 171–179.
57. Mama, R.; Jung, K.; Bidorn, B.; Namsai, M.; Feng, M. The local observed trends and variability in rainfall indices over the past century of the Yom River Basin, Thailand. *Journal of the Korean Society of Hazard Mitigation* **2018**, *18*, 41–55.
58. Li, Z.; Xu, X.; Yu, B.; Xu, C.; Liu, M.; Wang, K. Quantifying the impacts of climate and human activities on water and sediment discharge in a karst region of Southwest China. *Journal of Hydrology* **2016**, *542*, 836–849.
59. Searcy, J.K.; Hardison, H.H. *Double-Mass Curves, Manual of Hydrology: Part 1, General Surface Water Techniques*; US Geological Survey: Washington D.C., USA, 1960; pp. 1–66.
60. Gao, P.; Li, P.; Zhao, B.; Xu, R.; Zhao, G.; Sun, W.; Mu, X. Use of double mass curves in hydrologic benefit evaluations. *Hydrological Processes* **2017**, *31*, 4639–4646.

61. Thiessen, A.H. Precipitation averages for large areas. *Monthly Weather Review* **1911**, *39*, 1082–1084.
62. Moriasi, D.N.; Arnold, J.G.; Van Liew, M.W.; Bingner, R.L; Harmel, R.D.; Veith, T.L. Model evaluation guidelines for systematic quantification of accuracy in watershed simulations. *Hydrological Processes* **2007**, *50*, 885–900.
63. Bidorn, B.; Kish, S.A.; Donoghue, J.F.; Huang, W.; Bidorn, K. Variability of the total sediment supply of the Chao Phraya River, Thailand. River Sedimentation. In Proceedings of the 13th International Symposium on River Sedimentation, Stuttgart, Ger-many, 19–22 September 2016; CRC Press: Stuttgart, Germany, 2016.
64. Namsai, M.; Mama, R.; Sirapojanakul, S.; Chanyotha, S.; Phanomphongphaisan, N.; Bidorn, B. The characteristics of sediment transport in the upper and middle Yom River, Thailand. In Proceedings of the THA 2019 International Conference on Water Management and Climate Change towards Asia's Water-Energy-Food Nexus and SDGs, Bangkok, Thailand, 23–25 January 2019; Water Resources System Research Unit, Chulalongkorn University: Bangkok, Thailand, 2019; pp. 346–352.
65. Turowski, J.M.; Rickenmann, D.; Dadson, S.J. The partitioning of the total sediment load of a river into suspended load and bedload: A review of empirical data. Sedimentology 2010, 57, 1126–1146.
66. Royal Irrigation Department (RID). The Relation between Suspended Sediment and Drainage Area in 25 River Basins; Royal Irrigation Department: Bangkok, Thailand, 2012. (In Thai)
67. Wu, C.; Ji, C.; Shi, B.; Wang, Y.; Gao, J.; Yang, Y.; Mu, J. The impact of climate change and human activities on streamflow and sediment load in the Pearl River basin. *International Journal of Sediment Research* **2019**, *34*, 307–321.
68. Panda, D.K.; Kumar, A.; Mohanty, S. Recent trends in sediment load of tropical (Peninsular) river basins of India. *Global Planetary Change* **2011**, *75*, 108–118.
69. Li, D.; Lu, X.X.; Yang, X.; Chen, L.; Lin, L. Sediment load responses to climate variation and cascade reservoirs in the Yangtze River: A case study of the Jinsha River. *Geomorphology* **2018**, *322*, 41–52.
70. Guo, L.P.; Mu, X.M.; Hu, J.M.; Gao, P.; Zhang, Y.F.; Liao, K.T.; Bai, H.; Chen, X.L.; Song, Y.J.; Jin, N. Assessing impacts of climate change and human activities on streamflow and sediment discharge in the Ganjiang River Basin (1964–2013). *Water* **2019**, *11*, 1679.
71. Graf, W.L. Downstream hydrologic and geomorphic effects of large dams on America rivers. *Geomorphology* **2006**, *79*, 336–360.
72. Land Development Department (LDD). Status of soil erosion in Thailand; Land Development Department: Bangkok, Thailand, 2020. (In Thai)
73. Kitisuntorn, P. Sediment transport and navigation problem in lower Nan River. Dissertation, Doctor of Engineering, Department of Water Resources Engineering, Chulalongkorn University, Bangkok, Thailand, 1994. (In Thai)
74. Brune, G.M. Trap efficiency of reservoirs. *Eos, Transactions American Geophysical Union* **1953**, *34*(3), 407–418.